

Electron localization in a quasiperiodic array of potential wells

G. Wahlström and K. A. Chao

Department of Physics and Measurement Technology, University of Linköping, S-581 83 Linköping, Sweden

(Received 20 April 1988)

We have solved the Schrödinger equation for a potential consisting of an array of barriers the widths of which are modulated incommensurately. The Lyapunov exponent as a function of eigenenergy has been calculated to determine the localization properties of eigenstates in the entire spectrum. When the strength of the potential modulation is increased, the transition of the eigenstate from extended to localized character is energy dependent, in contrast to the energy-independent transition appearing in the Aubry model. In certain limits, our results reduce to those obtained by other authors using simplified models.

I. INTRODUCTION

About ten years ago Hofstadter¹ performed a numerical investigation on Harper's equation² and conjectured the rule of hierarchical band splittings of the energy spectrum. Soon after the discovery by Hofstadter, Aubry³ proposed an equivalent one-dimensional tight-binding model Hamiltonian for systems with incommensurate potentials,

$$H(Q) = \sum_{n=-\infty}^{\infty} [E(Q, n)a_n^\dagger a_n - t(a_{n+1}^\dagger a_n + a_{n-1}^\dagger a_n)], \quad (1)$$

where $E(Q, n) = V \cos(Q2\pi n)$ and Q is an irrational number. André and Aubry⁴ have demonstrated a novel property of the Aubry Hamiltonian (1) that all eigenfunctions are localized if $V > 2t$, and all eigenfunctions are extended if $V < 2t$. In the last ten years the Aubry Hamiltonian has been extensively studied by many authors.⁵⁻²⁰ Although interesting transport properties of the one-dimensional Aubry Hamiltonian have been predicted theoretically, unfortunately, so far there is no experimen-

tal confirmation.

The simplest model structure of a realistic system which may be described by the Aubry Hamiltonian is a three-dimensional lattice with incommensurate modulation of potential along one crystal axis.²¹ Recently we have used such a three-dimensional model to calculate the optical transmission spectrum of Rb_2ZnBr_4 and obtained good agreement with experimental data.²² The development of molecular-beam epitaxy techniques allows the fabrication of semiconductor superlattice crystals with layer thickness modulated along one crystal axis.²³ The effective-mass theory of pure bulk semiconductors has been applied to the study of plasma excitations in modulated semiconductor superlattices.^{24,25} However, in the presence of abrupt change of effective mass across sharp interfaces within a superlattice crystal, the validity of the conventional effective-mass Hamiltonian remains an open question.²⁶

While the tight-binding Hamiltonian (1) has received much attention, relatively little work was done on the other limiting case of a modulated one-dimensional array of potential barriers. The potential shown in Fig. 1 has the general form

$$V(x) = \begin{cases} 0 & \text{for } x_{n-1} < x < x_{n-1} + a_n = x_n - b_n, \\ U_n > 0 & \text{for } x_{n-1} + a_n < x < x_{n-1} + a_n + b_n = x_n, \end{cases} \quad (2)$$

with integer n between $-\infty$ and ∞ . One special form of $V(x)$ is a modulated array of delta-function barriers

$$V(x) = \sum_{n=-\infty}^{\infty} U_n \delta(x - x_n). \quad (3)$$

A further simplification is to assume a constant U for U_n , and to modulate the position x_n incommensurately according

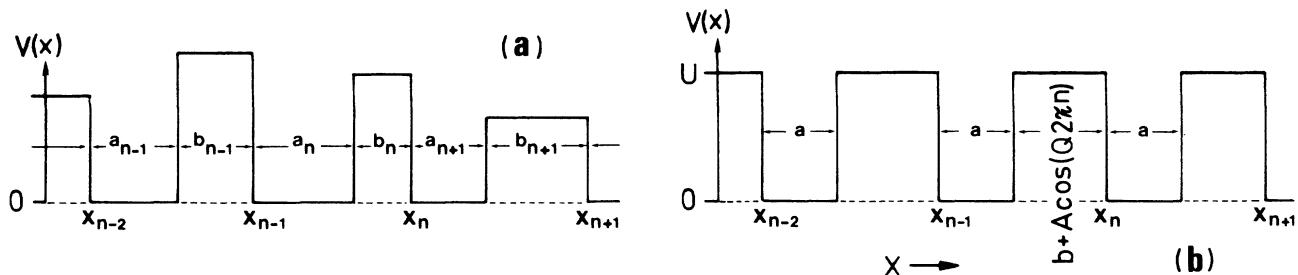


FIG. 1. Model potential (a) for Eq. (2), and (b) for Eq. (4).

to $A \cos(Q2\pi n)$. In this case the eigensolutions of the Schrödinger equation were studied,²⁷⁻²⁹ and in contrary to the characteristic feature of the Aubry model, there is no eigenenergy-independent transition from all extended to all localized eigenfunctions as the strength of modulation is increased.²⁹ Bellisard *et al.*³⁰ have investigated another simplified case of (3) with lattice positions $x_n = n$ but with U_n incommensurately modulated according to $A \cos(Q2\pi n)$. The resulting eigenvalue problem can be formally mapped into the Aubry Hamiltonian, which will be discussed in details in the next section.

In this paper we are interested in the eigenproperties of the potential

$$V(x) = \begin{cases} 0 & \text{for } x_{n-1} < x < x_{n-1} + a, \\ U > 0 & \text{for } x_{n-1} + a < x < x_{n-1} + a + b + A \cos(Q2\pi n) = x_n, \end{cases} \tag{4}$$

which is shown in Fig. 1. The energy spectrum of (4) was calculated earlier and exhibits a hierarchical band splittings.³¹ In the next section we will derive the recursion relation for (4) and map it into the recursion relation for the tight-binding Aubry model. The recursion relation will then be used in the rest of this paper to study the localization properties of the eigenstates.

We would like to point out that the potential (4) is commonly used to investigate the electronic properties of semiconductor superlattices, provided that the spatial dependence of the effective mass and the correct boundary conditions at the interface are properly taken into account.²⁶

II. TRANSFER MATRIX

We want to solve the one-dimensional Schrödinger equation

$$-d^2\psi(x)/dx^2 + V(x)\psi(x) = E\psi(x) \tag{5}$$

with the potential $V(x)$ given by (4). Here we have chosen the width of the potential well a as units of length and $(1/2m)(\hbar/a)^2$ as units of energy. Since for $E > U$ all states are extended, we will consider the energy region $0 < E < U$. The general solution of $\psi(x)$ can be expressed as

$$\psi(x) = \begin{cases} A_n \exp[i\kappa(x - x_n + b_n)] + B_n \exp[-i\kappa(x - x_n + b_n)] & \text{for } x_{n-1} < x < x_{n-1} + a, \\ C_n \exp[\gamma(x - x_n)] + D_n \exp[-\gamma(x - x_n)] & \text{for } x_{n-1} + a = x_n - b_n < x < x_n, \end{cases} \tag{6}$$

where $\kappa = \sqrt{E}$, $\gamma = \sqrt{U - E}$, and $b_n = b + A \cos(Q2\pi n)$. The continuity conditions on $\psi(x)$ and $d\psi(x)/dx$ at $x = x_{n-1}$ and at $x = x_n - b_n$ yield the transfer relation

$$\begin{pmatrix} C_n \\ D_n \end{pmatrix} = \begin{pmatrix} \left[\cos\kappa + \frac{1}{2} \left[\frac{\gamma - \kappa}{\kappa - \gamma} \right] \sin\kappa \right] \exp(\gamma b_n) & - \left[\frac{1}{2} \left[\frac{\gamma + \kappa}{\kappa + \gamma} \right] \sin\kappa \right] \exp(\gamma b_n) \\ \left[\frac{1}{2} \left[\frac{\gamma + \kappa}{\kappa + \gamma} \right] \sin\kappa \right] \exp(-\gamma b_n) & \left[\cos\kappa - \frac{1}{2} \left[\frac{\gamma - \kappa}{\kappa - \gamma} \right] \sin\kappa \right] \exp(-\gamma b_n) \end{pmatrix} \begin{pmatrix} C_{n-1} \\ D_{n-1} \end{pmatrix}. \tag{7}$$

The set of coefficients $\{D_n\}$ can be eliminated to derive a recursion relation of the C_n 's. If we define $\mathcal{C}_n = [\exp(\gamma\alpha_n)]C_n$ with

$$\alpha_n = -\frac{b}{2} - \frac{A \cos[Q\pi(2n + 1)]}{2 \cos(Q\pi)}, \tag{8}$$

then the set of coefficients $\{\mathcal{C}_n\}$ has the recursion relation

$$\begin{pmatrix} \mathcal{C}_n \\ \mathcal{C}_{n-1} \end{pmatrix} = \begin{pmatrix} \left[\cos\kappa + \frac{1}{2} \left[\frac{\gamma - \kappa}{\kappa - \gamma} \right] \sin\kappa \right] \exp(-2\gamma\alpha_{n-1}) + \left[\cos\kappa - \frac{1}{2} \left[\frac{\gamma - \kappa}{\kappa - \gamma} \right] \sin\kappa \right] \exp(+2\gamma\alpha_{n-2}) & -1 \\ 1 & 0 \end{pmatrix} \begin{pmatrix} \mathcal{C}_{n-1} \\ \mathcal{C}_{n-2} \end{pmatrix} \\ \equiv \mathbf{T}(n-1) \begin{pmatrix} \mathcal{C}_{n-1} \\ \mathcal{C}_{n-2} \end{pmatrix}. \tag{9}$$

There is a similar but much simpler recursion relation for the eigenfunctions of the Aubry Hamiltonian (1). If $\sum_{n=-\infty}^{\infty} f_n a_n^\dagger$ is the creation operator corresponding to an eigenstate of (1), then it is easy to derive the equation

$$\begin{pmatrix} f_n \\ f_{n-1} \end{pmatrix} = \begin{pmatrix} [E(Q, n-1) - E]/t & -1 \\ 1 & 0 \end{pmatrix} \begin{pmatrix} f_{n-1} \\ f_{n-2} \end{pmatrix} \equiv \mathbf{T}_A(n-1) \begin{pmatrix} f_{n-1} \\ f_{n-2} \end{pmatrix}, \tag{10}$$

where E is the eigenenergy. Although our modulated-potential model is mapped into the Aubry Hamiltonian in the sense that $\mathbf{T}(n)$ and $\mathbf{T}_A(n)$ are similar, there is an essential difference between the localization properties of the eigenstates of the two models. The origin of the difference can be demonstrated with a limiting case of the potential $V(x)$ given by (4). Let us define two finite parameters

$$\mathcal{A} = \lim_{b \rightarrow 0} (A/b) \tag{11}$$

and

$$\mathcal{U} = \lim_{b \rightarrow 0} (bU) . \tag{12}$$

Then, $V(x)$ reduces to an array of modulated delta potentials located at regular positions $x_n = na$. The strength of the delta potential at x_n is modulated according to $\mathcal{U}[1 + \mathcal{A} \cos(Q2\pi n)]$. In this case the (1,1) element of $\mathbf{T}(n)$ is simplified to

$$[\mathbf{T}_0(n)]_{11} = 2 \cos \kappa + \mathcal{U} \frac{\sin \kappa}{\kappa} [1 + \mathcal{A} \cos(Q2\pi n)] . \tag{13}$$

Bellisard *et al.*³⁰ have studied a similar modulated delta-potential model with the strength of the delta potential modulated according to $\mathcal{U} \cos(Q2\pi n)$. They have also derived the corresponding transfer matrix $\mathbf{T}_B(n)$ as (9). The (1,1) element of $\mathbf{T}_B(n)$ is

$$[\mathbf{T}_B(n)]_{11} = 2 \cos \kappa + \mathcal{U} \frac{\sin \kappa}{\kappa} \cos(Q2\pi n) . \tag{14}$$

By comparing $[\mathbf{T}_B(n)]_{11}$ and $[\mathbf{T}_A(n)]_{11}$, we see that the modulated delta-potential model is almost equivalent to the Aubry model, except that in $[\mathbf{T}_B(n)]_{11}$ the amplitude $V(E) = \mathcal{U}(\sin \kappa)/\kappa$ of the single-site energy modulation becomes dependent on the eigenenergy $E = \kappa^2$. The ratio $V(E)/t$ is then no longer a constant value throughout the entire spectrum as for the case of the Aubry model. Consequently, the modulated-potential model does not exhibit an eigenenergy-independent transition from all extended states to all localized states as the strength of modulation increases. This feature will be clearly demonstrated later in our numerical results.

III. ELECTRON LOCALIZATION

We have derived earlier the energy spectrum of the Schrödinger equation (5) with potential (4).³¹ It was shown that at a given stage of hierarchical band splitting, the characteristic feature of the spectrum is still preserved by the rational approximation $Q \simeq j/J$, where j and J are integers. Let us first demonstrate such characteristic energy spectrum with a numerical calculation. It was pointed out in the previous section that the interesting region of eigenenergy E lies between 0 and U . Within this region, there may exist more than one energy band for a pure periodic potential without incommensurate modulation ($A = 0$). For the present study, however, it is sufficient to have only one band in the energy range $0 < E < U$ when $A = 0$. Since we have chosen the width of the potential well a as units of length and

$(1/2m)(\hbar/a)^2$ as units of energy, the one-band situation when $A = 0$ can be achieved if we set the barrier height $U = 6$ and the barrier width $b = 1$. We would like to emphasize that these parameter values are chosen for convenience only, without qualitative influence on final conclusions of the present study.

When the potential barrier is modulated incommensurately, the modulated barrier-width must be positive. Therefore, the modulation amplitude A has the value between 0 and b ($b = 1$). For given values of the modulation amplitude A and the rationally approximated $Q = j/J$, the energy spectrum of (5) is obtained numerically. The spectra are shown in Fig. 2 for weak modulation $A = 0.3$ (upper part) and strong modulation $A = 0.8$ (lower part). In each case, we consider eight values of $Q = j/17$, where $j = 1, 2, \dots, 8$. The spectra exhibit the general feature that if we fix the value of A and increase the value of Q , the total width of the entire spectrum decreases if Q is not very large. On the other hand, when we fix Q and increase A , the total width of the entire spectrum and each individual gap increase, but the width of every subband decreases. Consequently, as the modulation amplitude grows the spectrum approaches a point-spectrum and the corresponding eigenstates becomes more localized.

Whether an eigenstate with eigenenergy E is localized or not can be estimated by its Lyapunov exponent defined as

$$\Gamma(E) = \lim_{N \rightarrow \infty} \left\{ \frac{1}{N} \ln \{ \text{norm}[\mathbf{T}(N)\mathbf{T}(N-1) \cdots \mathbf{T}(2)\mathbf{T}(1)] \} \right\} . \tag{15}$$

Oseledec³² and Avron and Simon³³ have proved that an eigenstate is exponentially localized if the corresponding $\Gamma(E) \neq 0$. If $\Gamma(E) = 0$, then the eigenstate may be extended. Based on this criterion André and Aubry⁴ have

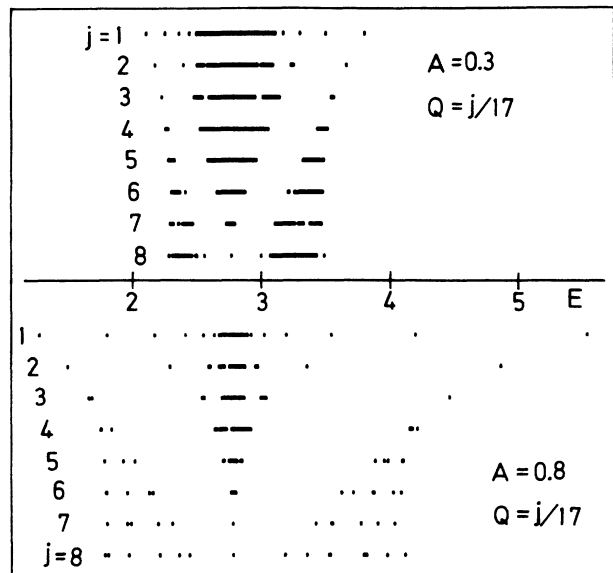


FIG. 2. Energy spectra for rationally approximated wave number $Q = j/17$. Black horizontal segments are subbands.

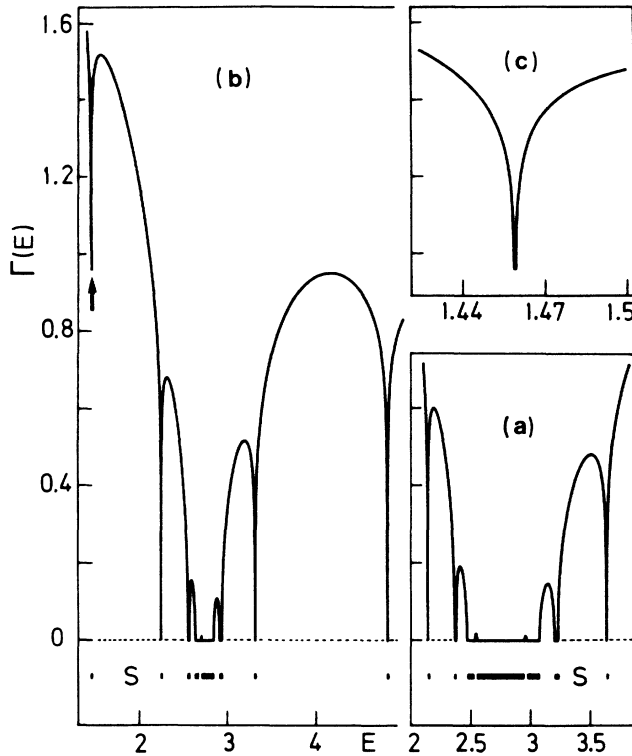


FIG. 3. Lyapunov exponent $\Gamma(E)$ for $Q = \frac{2}{17}(6.3/2\pi)$ with modulation amplitude (a) $A=0.3$ and (b) $A=0.8$. All plots have same vertical scale marked at the left. Corresponding spectra are indicated by S .

shown the metal-insulator transition in the Aubry model.

We have calculated the Lyapunov exponents for various modulations, and found convergent results when $N > 5000$. Figure 3 shows the value of $\Gamma(E)$ for $Q = \frac{2}{17}(6.3/2\pi)$ with $A=0.3$ [panel (a)] and $A=0.8$ [panel (b)]. The corresponding spectrum of each case is plotted at the bottom of the same panel and is marked as S . Both panel (a) and panel (b) have same vertical scale which is labeled at the left side of panel (b). When $A=0.3$, we seen in panel (a) that $\Gamma(E)$ is finite only if E lies in energy gaps and so is not an eigenenergy. Therefore, in the case of weak modulation all eigenstates are extended.

As the modulation amplitude increases, one expects localized states emerging first at the lower end of the energy spectrum. It is indeed so, as demonstrated by panel (b) of Fig. 3 for $A=0.8$. For all states in the lowest subband, $\Gamma(E)$ has large finite values. The behavior of $\Gamma(E)$ in the region marked by the arrow is illustrated in panel (c) with an expanded energy scale.

The calculated $\Gamma(E)$ for $Q = \frac{6}{17}(6.3/2\pi)$ is shown in Fig. 4 with $A=0.3$ [panel (a)], $A=0.5$ [panel (b)], and $A=0.8$ [panel (d)]. In each case the corresponding energy spectrum is also plotted and marked as S . For weak modulation $A=0.3$, again all eigenstates are extended. When A increases to 0.5, localized states begin to appear at the lower part of the spectrum. With further increase of A to 0.8, eigenstates at the higher part of the spectrum

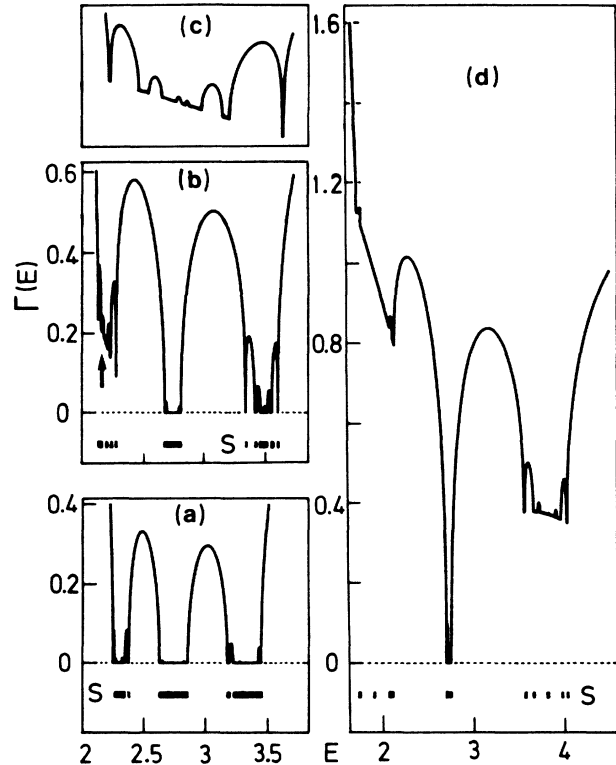


FIG. 4. Lyapunov exponent $\Gamma(E)$ for $Q = \frac{6}{17}(6.3/2\pi)$ with modulation amplitude (a) $A=0.3$, (b) $A=0.5$, and (d) $A=0.8$. Panels (a) and (b) have same horizontal energy scale. Corresponding spectra are indicated by S .

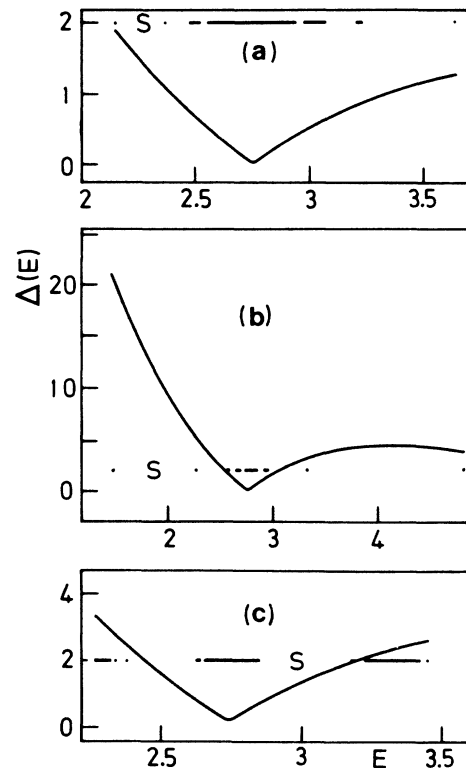


FIG. 5. Effective amplitude $\Delta(E)$ for (a) $(Q; A) = (\frac{2}{17}(6.3/2\pi); 0.3)$, (b) $(Q; A) = (\frac{2}{17}(6.3/2\pi); 0.8)$, and (c) $(Q; A) = (\frac{6}{17}(6.3/2\pi); 0.3)$. Corresponding spectra are indicated by S .

are also localized, leaving a small region at the middle of the spectrum for extended eigenstates. From our numerical results we have also detected regular fine structure of $\Gamma(E)$ when E lies in the localized region. In panel (c) we plot with expanded horizontal scale the part of the $\Gamma(E)$ curve marked by the arrow in panel (b). This plot in panel (c) clearly indicates that the $\Gamma(E)$ for localized states in subbands varies linearly with the eigenenergy E . The significance of such linear behavior needs further investigation.

$$\exp \left[\frac{A\gamma}{\cos(Q\pi)} \cos[Q\pi(2n+1)] \right] = I_0 \left[\frac{A\gamma}{\cos(Q\pi)} \right] + 2 \sum_{m=1}^{\infty} I_m \left[\frac{A\gamma}{\cos(Q\pi)} \right] \cos[mQ\pi(2n+1)], \quad (16)$$

where $I_m(x)$ is the modified Bessel function. If both A and Q are small, the argument of the modified Bessel function is small and so the series expansion of (16) converges rapidly. If A and Q are sufficiently small, we can neglect all terms in (16) for which $m > 1$. Then the modulation term in $[\mathbf{T}(n)]_{11}$ is simply a cosine function

$$I_1 \left[\frac{A\gamma}{\cos(Q\pi)} \right] \cos[Q\pi(2n+1)].$$

IV. AUBRY MODEL AS A LIMITING CASE

We have emphasized the similarity between the recursion relation (9) for the present model and the recursion relation (10) for the Aubry model. Now we would like to show that (10) is a limiting case of (9) when both A and Q are small.

The $[\mathbf{T}(n)]_{11}$ element of (9) contains exponential functions of cosine functions. Such exponential functions can be expanded as, for example,

This is just the case of the Aubry model.

Under the approximation of keeping only the $I_1(x)$ term in the series, $[\mathbf{T}(n)]_{11}$ can be readily expressed as

$$[\mathbf{T}(n)]_{11} \simeq \Delta_0 + \Delta \cos[Q\pi(n-1)], \quad (17)$$

where Δ_0 is a function of energy, and

$$\Delta = 2I_1 \left[\frac{A\gamma}{\cos(Q\pi)} \right] \left\{ e^{2\gamma b} \left[\cos\kappa + \frac{1}{2} \left[\frac{\gamma}{\kappa} - \frac{\kappa}{\gamma} \right] \sin\kappa \right]^2 + e^{-2\gamma b} \left[\cos\kappa - \frac{1}{2} \left[\frac{\gamma}{\kappa} - \frac{\kappa}{\gamma} \right] \sin\kappa \right]^2 - 2 \left[\cos\kappa + \frac{1}{2} \left[\frac{\gamma}{\kappa} - \frac{\kappa}{\gamma} \right] \sin\kappa \right] \left[\cos\kappa - \frac{1}{2} \left[\frac{\gamma}{\kappa} - \frac{\kappa}{\gamma} \right] \sin\kappa \right] \cos(Q2\pi) \right\}^{1/2}. \quad (18)$$

To check the validity of the approximation (17), we can use the condition derived by André and Aubry⁴ that if $\Delta > 2$ (or $\Delta < 2$) the corresponding eigenstate is localized (or extended). We have calculated Δ for various values of A and Q . Figure 5 shows Δ as a function of E for $(Q; A) = (\frac{2}{17}(6.3/2\pi); 0.3)$ by panel (a), $(Q; A) = (\frac{2}{7}(6.3/2\pi); 0.8)$ by panel (b), and $(Q; A) = (\frac{6}{17}(6.3/2\pi); 0.3)$ by panel (c). In each case the corresponding energy spectrum is plotted along $\Delta = 2$ and is marked with S . When both A and Q are small, in panel (a) we see that $\Delta < 2$ for the entire spectrum and so all states are extended, in agreement with the exact result in panel (a) in Fig. 3. When A (or Q) increases, the value of Δ in panel (b) [or panel (c)] of Fig. 5 becomes greater than 2 in regions of both lower and higher energy. Then, localized states appear near both edges of each spectrum, in contradiction to the exact results given by panel (b) of Fig. 3 and panel (a) of Fig. 4.

V. FINAL REMARKS

We have derived the exact eigensolutions of an array of potential barriers with widths modulated incommensu-

ately. When the modulation amplitude A and/or the modulation wave number Q increase from zero, localized states first appear in the lower part of the spectrum, and then in the upper part of the spectrum. The transition from extended states to localized states is then energy dependent, different from the characteristic behavior of the Aubry model.

It is well known that the existence of superperiodicities in systems with incommensurate potentials makes the calculation of electrical conductivity a nontrivial problem.³⁴ A study of the transport properties will certainly provide better understanding of the present model.

ACKNOWLEDGMENTS

This work was supported by the Swedish Natural Science Research Council under Grant No. NRF-FFU-3996-140.

- ¹D. R. Hofstadter, *Phys. Rev. B* **14**, 2239 (1976).
²P. G. Harper, *Proc. Phys. Soc. London, Sect. A* **68**, 874 (1955).
³S. Aubry, in *Solid State Science: Solitons and Condensed Matter Physics*, edited by A. P. Bishop and T. Schneider (Springer, Berlin, 1978), Vol. 8, p. 264.
⁴S. Aubry and C. Andre, *Israel Phys. Soc.* **3**, 133 (1980).
⁵J. B. Sokoloff, *Phys. Rev. B* **23**, 6422 (1981).
⁶J. B. Sokoloff, *Solid State Commun.* **40**, 633 (1981).
⁷J. B. Sokoloff and J. V. Jose, *Phys. Rev. Lett.* **49**, 334 (1982).
⁸J. Bellissard, D. Bessis, and P. Moussa, *Phys. Rev. Lett.* **49**, 701 (1982).
⁹J. Bellissard and S. Simon, *J. Funct. Anal.* **48**, 408 (1982).
¹⁰M. Kohmoto, *Phys. Rev. Lett.* **51**, 1198 (1983).
¹¹I. M. Suslov, *Zh. Eksp. Teor. Fiz.* **84**, 1792 (1983) [*Sov. Phys.—JETP* **57**, 1044 (1983)].
¹²D. J. Thouless, *Phys. Rev. B* **28**, 4272 (1983).
¹³D. J. Thouless and Q. Niu, *J. Phys. A* **16**, 1911 (1983).
¹⁴S. Ostlund and R. Pandit, *Phys. Rev. B* **29**, 1394 (1984).
¹⁵M. Wilkinson, *Proc. R. Soc. London, Sect. A* **391**, 305 (1984).
¹⁶K. A. Chao, R. Riklund, and G. Wahlström, *J. Phys. A* **18**, L403 (1985).
¹⁷K. A. Chao, *J. Phys. A* **19**, 2907 (1986).
¹⁸K. A. Chao and G. Wahlström, *J. Phys. A* **20**, L71 (1987).
¹⁹K. A. Chao, *J. Phys. A* **20**, L709 (1987).
²⁰R. B. Stinchcombe and S. C. Bell, *J. Phys. A* **20**, L739 (1987).
²¹J. B. Sokoloff, *Phys. Rev. B* **22**, 5823 (1980).
²²G. Wahlström and K. A. Chao, *Phys. Rev. B* **36**, 9753 (1987).
²³R. Merlin, K. Bajema, R. Clarke, F.-Y. Juang, and P. K. Bhattacharya, *Phys. Rev. Lett.* **55**, 1768 (1985).
²⁴S. Das Sarma, A. Kobayashi, and R. E. Prange, *Phys. Rev. Lett.* **56**, 1280 (1986).
²⁵P. Hawrylak and J. J. Quinn, *Phys. Rev. Lett.* **57**, 380 (1986).
²⁶R. A. Morrow, *Phys. Rev. B* **35**, 8074 (1987).
²⁷M. Ya. Azbel, *Phys. Rev. Lett.* **43**, 1954 (1979).
²⁸M. Ya. Azbel and M. Rubinstein, *Phys. Rev. B* **27**, 6530 (1983).
²⁹C. de Lange and T. Janssen, *Phys. Rev. B* **28**, 195 (1983).
³⁰J. Bellissard, A. Formoso, R. Lima, and D. Testard, *Phys. Rev. B* **26**, 3024 (1982).
³¹G. Wahlström and K. A. Chao, *J. Phys. A* **21**, L135 (1988).
³²V. I. Oseledec, *Trudy. Mosk. Mat. Obsc.* **19**, 679 (1968).
³³J. H. Avron and B. Simon, *Duke Math. J.* **50**, 369 (1983).
³⁴Youyan Liu and K. A. Chao, *Phys. Rev. B* **34**, 5247 (1986).